Target specificity among canonical nuclear poly(A) polymerases in plants modulates organ growth and pathogen response

Son Lang Vi[a,b,1], Gerda Trost[a], Peggy Lange[a], Hjördis Czesnick[a], Nishta Rao[c,2], Diana Lieber[d,3], Thomas Laux[d], William M. Gray[e], James L. Manley[c], Detlef Groth[a], Christian Kappel[a], and Michael Lenhard[a,4]

[a]Institut für Biochemie und Biologie, Universität Potsdam, 14476 Potsdam, Germany; [b]Department of Cell and Developmental Biology, John Innes Centre, Norwich NR4 7UH, United Kingdom; [c]Department of Biological Sciences, Columbia University, New York, NY 10027; [d]BIOSS Center for Biological Signaling Studies, Albert-Ludwigs-Universität Freiburg, 79104 Freiburg, Germany; and [e]Department of Plant Biology, University of Minnesota, St. Paul, MN 55108

Edited by David C. Baulcombe, University of Cambridge, Cambridge, United Kingdom, and approved July 9, 2013 (received for review March 1, 2013)

Polyadenylation of pre-mRNAs is critical for efficient nuclear export, stability, and translation of the mature mRNAs, and thus for gene expression. The bulk of pre-mRNAs are processed by canonical nuclear poly(A) polymerase (PAPS). Both vertebrate and higher-plant genomes encode more than one isoform of this enzyme, and these are coexpressed in different tissues. However, in neither case is it known whether the isoforms fulfill different functions or polyadenylate distinct subsets of pre-mRNAs. Here we show that the three canonical nuclear PAPS isoforms in *Arabidopsis* are functionally specialized owing to their evolutionarily divergent C-terminal domains. A strong loss-of-function mutation in *PAPS1* causes a male gametophytic defect, whereas a weak allele leads to reduced leaf growth that results in part from a constitutive pathogen response. By contrast, plants lacking both *PAPS2* and *PAPS4* function are viable with wild-type leaf growth. Polyadenylation of *SMALL AUXIN UP RNA* (*SAUR*) mRNAs depends specifically on *PAPS1* function. The resulting reduction in *SAUR* activity in *paps1* mutants contributes to their reduced leaf growth, providing a causal link between polyadenylation of specific pre-mRNAs by a particular PAPS isoform and plant growth. This suggests the existence of an additional layer of regulation in plant and possibly vertebrate gene expression, whereby the relative activities of canonical nuclear PAPS isoforms control de novo synthesized poly(A) tail length and hence expression of specific subsets of mRNAs.

The poly(A) tail at the 3′ end is an essential feature of virtually all eukaryotic mRNAs that influences stability, nuclear export, and translational efficiency of the mRNAs (1, 2). It is synthesized after RNA polymerase II has transcribed past the cleavage and polyadenylation site and associated signal sequences (3, 4). These sequences are bound by several protein complexes, including Cleavage-stimulation Factor (CstF) and Cleavage and Polyadenylation Specificity Factor (CPSF) in animals and their counterparts in yeast and presumably in plants (2, 5). The complexes cleave the nascent pre-mRNA at the prospective polyadenylation site and recruit poly(A) polymerase (PAPS) to add the poly(A) tail.

The poly(A) tail is synthesized by PAPSs, with the bulk of cellular pre-mRNAs being polyadenylated by canonical nuclear PAPSs (cPAPSs) (5, 6) that share substantial sequence identity with human poly(A) polymerase-α (PAPOLA), bovine poly(A) polymerase, or the yeast enzyme Pap1p (7–9). Although the *Saccharomyces cerevisiae* and *Drosophila melanogaster* genomes only encode one cPAPS, which is essential for growth (7, 10), three such cPAPSs are found in humans: PAPOLA (PAPα), PAPOLB (PAPβ), and PAPOLG (PAPγ) (11). Of these, PAPOLA is thought to be the main PAPS in somatic cells. PAPOLA and PAPOLG proteins contain a C-terminal regulatory region next to the highly conserved catalytic N-terminal domain and are found either in both nucleus and cytoplasm (PAPOLA) or only in the nucleus (PAPOLG) of cells throughout the human body (9, 11–14). By contrast, PAPOLB lacks the C-terminal region, is exclusively cytoplasmic, and is only found in testis cells, where it is required to extend the poly(A) tail of cytoplasmic mRNAs encoding sperm-related proteins (15); as a consequence, male mice mutant for *PAPOLB* are sterile.

The *Arabidopsis thaliana* genome encodes four cPAPS proteins, termed PAPS1 to PAPS4 (16, 17). PAPS3 resembles PAPOLB in lacking an extended C-terminal region, being localized in the cytoplasm and expressed mainly in the male gametophytes (the pollen). By contrast, PAPS1, PAPS2, and PAPS4 all contain an extended C-terminal region, localize exclusively to the nucleus, and are expressed throughout the plant (2, 16–18). All four proteins have nonspecific polyadenylation activity in vitro, suggesting that they represent functional cPAPSs (16, 19). On the basis of the failure to identify homozygous transfer DNA (T-DNA) insertion mutants for any of the three genes, it was concluded that all of them are essential for plant growth and development (17).

Gene expression can be regulated via a number of mechanisms impinging on the mRNA 3′ end. The choice between alternative 3′ end cleavage sites is widely used to regulate gene expression in both animal and plant development, for example via the exclusion or inclusion of microRNA target sites in the resulting 3′ UTRs (20–24). Additionally, modulating the length of the poly (A) tails on mRNAs in the cytoplasm by the opposing actions of cytoplasmic PAPS (e.g., PAPOLB) and deadenylases can be used to control the expression of the encoded proteins (1, 15). However, it is currently unclear whether polyadenylation by nuclear cPAPS can also contribute to the control of specific gene expression. In principle, this could occur in either of two ways. First, pre-mRNAs could be differentially sensitive to variations in the total cPAPS activity provided by one or more functionally interchangeable cPAPS isoforms; such a mechanism may underlie specific developmental phenotypes in weak mutants of *D. melanogaster* cPAPS (25). Second, some mRNAs may be exclusively or preferentially polyadenylated by one cPAPS in organisms with more than one isoform. Given such target specificity,

Author contributions: S.L.V., G.T., C.K., and M.L. designed research; S.L.V., G.T., P.L., H.C., N.R., and M.L. performed research; D.L., T.L., and W.M.G. contributed new reagents/analytic tools; S.L.V., G.T., J.L.M., D.G., C.K., and M.L. analyzed data; and S.L.V. and M.L. wrote the paper.

The authors declare no conflict of interest.

This article is a PNAS Direct Submission.

Data deposition: The data reported in this paper have been deposited in the Gene Expression Omnibus (GEO) database, www.ncbi.nlm.nih.gov/geo (accession no. GSE48821).

[1]Present address: Cold Spring Habor Laboratory, Cold Spring Harbor, NY 11724.

[2]Present address: Kadmon Research Institute, New York, NY 10016.

[3]Present address: Institute of Virology, Ulm University Medical Center, 89081 Ulm, Germany.

[4]To whom correspondence should be addressed. E-mail: michael.lenhard@uni-potsdam.de.

This article contains supporting information online at www.pnas.org/lookup/suppl/doi:10.1073/pnas.1303967110/-/DCSupplemental.

modulating the balance of activities between the isoforms could then be used to alter the length of the de novo synthesized poly(A) tails, and hence ultimately gene expression, of subsets of mRNAs. Target specificity has at present only been observed for non-canonical PAPS (6, 26), such as Star-PAP, which is required for the cellular response to oxidative stress.

Here we provide evidence for functional specialization and target specificity among *A. thaliana* nuclear cPAPS isoforms. Mutations affecting different isoforms cause very different phenotypes that depend on the divergent C-terminal domains of the proteins. In particular, reduction of *PAPS1* activity disrupts polyadenylation of *SMALL AUXIN UP RNA* (*SAUR*) mRNAs and causes leaf growth defects due to reduced *SAUR* function and a constitutive pathogen response. We propose that this specificity of PAPS isoforms provides an additional level of regulating plant gene expression.

Results and Discussion

***paps1* Mutants Show Organ-Specific Effects on Growth.** From an ethyl-methanesulfonate (EMS) mutagenesis screen, we identified a unique recessive mutation causing opposite effects on the growth of leaves and flowers, termed *paps1-1* (Fig. 1 *A*–*C*). Although the size of *paps1-1* mutant leaves is reduced to less than one-third of the wild-type value, mutant petals and other floral organs are larger than in wild type, with petals reaching almost twice the wild-type size. At the cellular level, the reduced leaf size is largely due to a defect in cell expansion (Fig. 1*C*). Conversely, the size of *paps1-1* mutant petal cells is only increased by 21%, indicating that the bulk of the difference in petal size is due to a higher number of cells (Fig. 1*C*). Thus, *PAPS1* function is required to allow normal cell expansion in leaves and to limit cell proliferation in petals.

The *paps1-1* Mutation Reduces the Activity of PAPS1 in Canonical Nuclear Polyadenylation of pre-mRNAs. To determine the molecular basis of the *paps1-1* mutant phenotype, we isolated the affected gene by mapping and sequencing of candidate genes. This identified a C-to-T transition typical for EMS-induced mutations in the *At1g17980* gene coding for PAPS1 (Fig. S1*A*). The mutation causes an amino acid substitution of serine for proline at position 313. The mutated proline lies in a linker peptide between the nucleotidyl-transferase domain and the RNA-binding domain within the N-terminal catalytic region of the protein and is very highly conserved in PAPSs from yeast, plants, and animals (Fig. S1*B*). Complementation of the *paps1-1* mutant with a wild-type genomic copy of the *PAPS1* locus restored a wild-type phenotype (Fig. S1*C*). The *paps1-1* allele is temperature sensitive (Fig. S1*D*); in contrast to growth at 23 °C, seedlings grown at 28 °C showed a very severe phenotype with bleaching and almost complete growth inhibition, indicating that the phenotypes seen at lower temperatures result from only a moderate reduction in *PAPS1* activity (see also below).

To determine the effect of the *paps1-1* mutation on the protein's activity, we performed in vitro polyadenylation assays using purified recombinant protein (27). Whereas the wild-type protein showed robust polyadenylation activity, virtually no enzymatic activity was observed when using the mutant form (Fig. 1*D* and Fig. S1*E*).

To genetically determine whether PAPS1 is indeed involved in canonical pre-mRNA processing in the nucleus, we combined the *paps1-1* allele with a mutant allele of the *CSTF64* locus encoding the sole *A. thaliana* homolog to the Cstf64 subunit of the cleavage-stimulation factor complex (28). We could not recover any double homozygous *cstf64-1 paps1-1* mutants, and the siliques from *cstf64-1/+; paps1-1/paps1-1* plants contained 25% aborted seeds (Fig. 1*E* and Fig. S1*F*), indicating that the double mutant genotype confers embryo lethality. This contrasts with full seed set in either single mutant. Together, this synthetic lethality

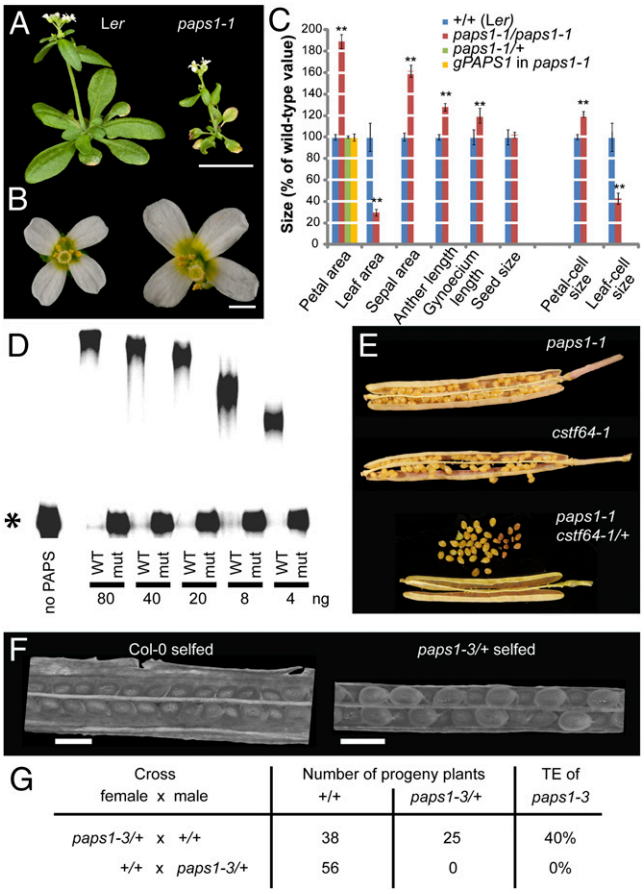

Fig. 1. Loss of *PAPS1* function leads to altered organ growth. (*A* and *B*) Whole-plant (*A*) and flower images (*B*) of the indicated genotypes. (*C*) Quantification of organ and cell sizes from the indicated genotypes. Values are mean ± SE from at least 5 (leaves), 20 (petals, sepals, anthers), 7 (gynoecia), or 55 (seeds) organs per genotype, normalized to the wild-type mean. (*D*) Autoradiograph of in vitro nonspecific polyadenylation assay. The indicated amounts of wild-type PAPS1 protein (WT) or of the mutant form encoded by the *paps1-1* allele (mut) were used. Asterisk indicates the unpolyadenylated RNA substrate. (*E*) Micrographs of opened siliques from the indicated genotypes. Note the aborted seeds produced by *paps1-1 cstf64-1/+* plants. (*F*) Light micrographs of opened siliques from Col-0 (*Left*) and *paps1-3/+* heterozygous plants (*Right*) after selfing. (*G*) Transmission efficiency (TE) of the *paps1-3* mutant allele through the male and the female gametophyte. The result for the first cross is not significantly different from the expected 50:50 ratio ($P = 0.10$, χ^2 test). (Scale bars, 1 cm in *A*, 1 mm in *B*, 500 μm in *F*.)

and the results of the in vitro assay strongly suggest that the *paps1-1* mutation affects nuclear polyadenylation of transcripts.

***PAPS1* Activity Is Essential for Male Gametophyte Function.** To determine the effects of a complete loss of *PAPS1* activity, we studied a presumed null allele with a T-DNA insertion in the fifth intron within the region coding for the N-terminal catalytic protein domain (*paps1-3*; Fig. S1*A*). It was not possible to recover plants homozygous for the *paps1-3* allele. To determine whether this is due to embryonic lethality or to a gametophytic defect, we analyzed the seeds developing on *paps1-3/+* heterozygous plants and performed reciprocal crosses. There was no evidence for either embryo lethality or a female gametophytic defect from analyzing the siliques of *paps1-3/+* plants, because we did not detect aborted seeds or unfertilized ovules (Fig. 1*F*). Consistent with this, the *paps1-3* mutant allele was normally transmitted through the female gametophyte (Fig. 1*G*). By contrast,

when applying pollen from *paps1-3*/+ plants to wild-type stigmas, none of the progeny carried the mutant allele (Fig. 1*G*), indicating that the *paps1-3* mutation causes a male gametophytic defect. Pollen from *paps1-1* mutant plants and from *paps1-3*/+ heterozygotes was morphologically normal and viable (Fig. S1*G*).

Thus, *PAPS1* represents an essential gene for male gametophyte function, and a progressive reduction of remaining *PAPS1* activity in the diploid sporophyte causes increasingly more severe phenotypic defects as seen in the *paps1-1* allele (see above).

The Three Canonical Nuclear Poly(A) Polymerases Encoded by the *A. thaliana* Genome Are Functionally Specialized. To determine the roles of the other two canonical nuclear PAPSs in *A. thaliana*, putative null alleles were isolated for *PAPS2* and *PAPS4*. In both cases the eighth exon within the region coding for the catalytic N-terminal domain was disrupted, and no full-length mRNA could be detected from the mutant alleles (Fig. S2 *B*, *D*, and *E*). Both single mutants and the *paps2-1 paps4-1* double mutant were viable (Fig. S2*B*) and showed normal leaf and petal growth (Fig. 2 *A* and *B*). To test whether the much more severe phenotypes resulting from loss of *PAPS1* function were simply due to *PAPS1* being responsible for most polyadenylation in *Arabidopsis*, we determined bulk poly(A) tail lengths in *paps1-1* mutant and wild-type seedlings. There was virtually no change in the distribution of bulk poly(A) tail lengths (Fig. S2 *F* and *G*), despite the very severe mutant phenotype under the growth conditions used (Fig. S1*D*). Together, these results indicate that most transcripts can be redundantly polyadenylated by either PAPS1 or PAPS2/PAPS4 but that a small subset of critical transcripts is exclusively or preferentially targeted by PAPS1.

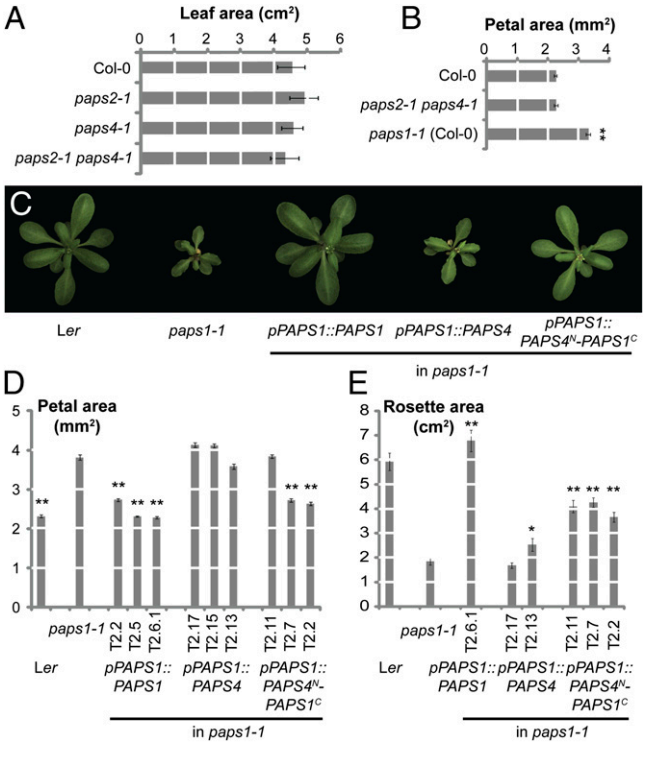

Fig. 2. The three nuclear PAPS isoforms in *A. thaliana* fulfill distinct functions. (*A* and *B*) Quantification of leaf (*A*) and petal size (*B*) in the indicated genotypes. Values are mean ± SE from at least five leaves and 20 petals per genotype. **Significantly different from wild-type value at $P < 0.01$ (*t* test). (*C*) Top views of plants of the indicated genotypes. (*D* and *E*) Quantification of petal (*D*) and rosette (*E*) size in the indicated genotypes. Individual bars represent independent transformant lines for the transgenic plants. Values are mean ± SE from at least 15 petals and at least six rosettes per genotype. Asterisks (*,**) indicate significant difference from *paps1-1* mutant value at $P < 0.05$ (*) or $P < 0.01$ (**) according to *t* test with Bonferroni correction.

The three proteins PAPS1, PAPS2, and PAPS4 share highly conserved N-terminal catalytic regions, whereas the C-terminal domains are more divergent (Fig. S2*A*). We therefore asked whether the functional divergence apparent from the different mutant phenotypes was due to differences at the protein level. Introducing the *PAPS4* coding region under the control of the *pPAPS1* promoter (*pPAPS1::PAPS4*) into a *paps1-1* background did not complement the mutant phenotype (Fig. 2 *C*–*E* and Fig. S2*C*). By contrast, when a chimeric protein consisting of the catalytic domain from PAPS4 and the C-terminal region from PAPS1 was expressed under the control of the *pPAPS1* promoter in *paps1-1* mutants (*pPAPS1::PAPS4*^{N}*-PAPS1*^{C}), it was able to substantially rescue the growth phenotype in leaves and particularly in flowers (Fig. 2 *C*–*E* and Fig. S2*C*). Thus, divergence in the C-terminal domains of the proteins is responsible for functional specialization among the PAPS isoforms in *A. thaliana*.

Polyadenylation of *SAUR* mRNAs Is Defective in *paps1* Mutants. To determine the molecular basis for the *paps1* mutant phenotypes, we compared transcript abundances in *paps1-1* mutant vs. wild-type leaves and flowers, using microarray hybridization. A total of 1,130 and 779 genes were misregulated more than twofold in *paps1-1* mutant leaves and flowers compared with wild type, respectively (Tables S1 and S2). Two hundred sixty-one genes were misregulated in both organs, suggesting that despite a substantial overlap in the molecular phenotypes of mutant leaves and floral organs, many transcript changes were specific to one or the other organ type, potentially contributing to the different growth phenotypes.

We found a significantly reduced hybridization signal for the family of *SAUR* mRNAs (29–31) from *paps1-1* mutants compared with wild type, particularly in seedlings (Fig. 3*A* and Fig. S3*A*; median and average fold-change of 0.72). This was not accompanied by a comparable misregulation of other auxin-responsive genes, such as *Aux/IAA* or *GH3* family members (Fig. 3*A* and Fig. S3*A*), indicating that the *paps1-1* mutation did not interfere with auxin response as such. Testing individual *SAUR* transcripts using quantitative RT-PCR (qRT-PCR) with oligo (dT) priming confirmed the reduced signal specifically from *paps1-1* mutants but not from *paps2-1 paps4-1* mutants (Fig. 3*B*). However, no such effect was observed when using random hexamers to prime the reverse transcription, with comparable or even higher signals in *paps1-1* mutants than in wild type (Fig. 3*B*). This suggests that the weaker signal on the microarrays and in the oligo(dT)-primed qRT-PCR was due to less efficient oligo (dT)-primed reverse transcription because of a shorter poly(A) tail, not due to reduced abundance of the tested *SAUR* mRNAs.

To determine whether *PAPS1* activity was indeed required for polyadenylation of *SAUR* mRNAs, we compared their poly(A) tail lengths between *paps1-1* mutants and wild type using a PCR-based assay to amplify part of the coding sequence/3′ UTR and the entire poly(A) tail (*SI Results and Discussion*). Before harvesting, seedlings were kept at 30 °C for 2 h to largely abolish the remaining activity of the temperature-sensitive mutant protein (see above). PCR products for *SAUR19/24* and *SAUR62/63/66/68* mRNAs from *paps1-1* mutants were shorter than from wild type or *paps2 paps4* double mutants (Fig. 3 *C* and *D*, Fig. S3 *D* and *E*, and *SI Results and Discussion*). To confirm that the different lengths of the PCR products indeed reflected a difference in poly (A) tail length and not in the choice of cleavage site, we subcloned and sequenced individual molecules. This indicated that the choice of 3′ end cleavage site was not affected (Fig. S3 *B* and *G*) and confirmed the dramatic reduction in the lengths of the poly(A) tails specifically in *paps1-1* mutants but not in *paps2-1 paps4-1* plants (Fig. 3*E* and Fig. S3*F*). The median lengths of poly(A) tails determined from subcloned molecules from wild

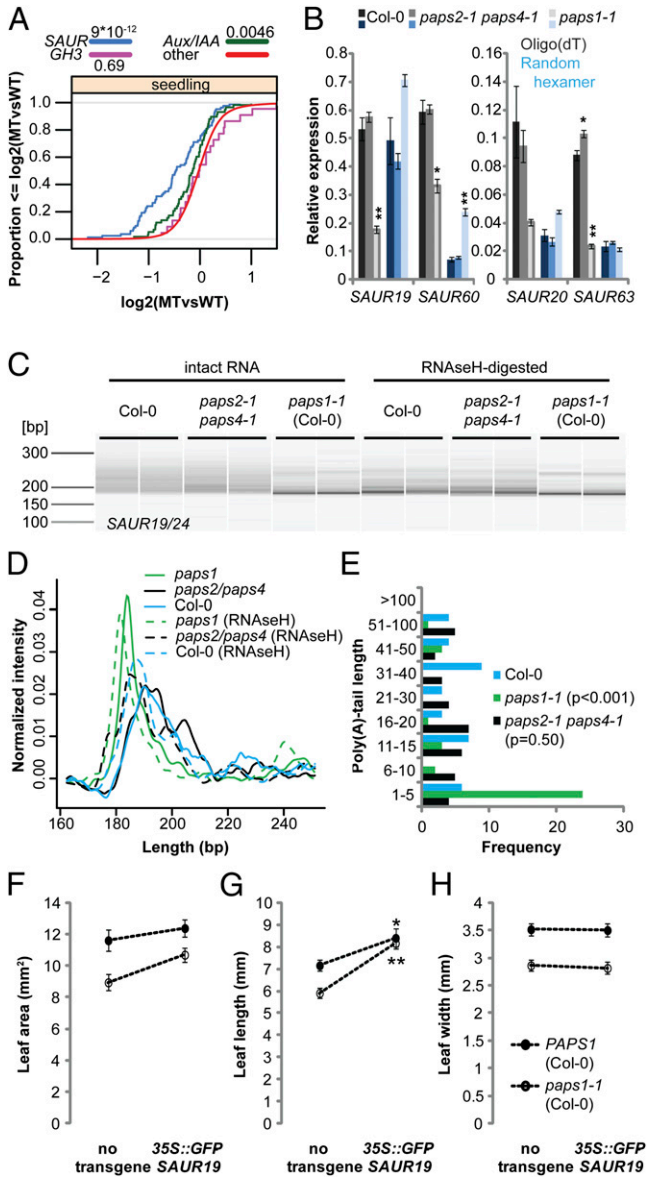

Fig. 3. Defective polyadenylation of *SAUR* mRNAs in *paps1* contributes to reduced leaf growth. (*A*) Cumulative distribution plot of the expression levels of *SAUR*, *GH3*, and *Aux/IAA* family members in *paps1-1* vs. wild-type seedlings. The *y* axis indicates the fraction of genes with a log2-expression ratio less than or equal to the value on the *x* axis. Numbers in legend are *P* values of a Wilcoxon rank-sum test. "other," all remaining genes on the array. (*B*) Expression of the indicated *SAUR* genes in *paps1-1* and *paps2-1 paps4-1* mutant seedlings compared with wild-type. Values from oligo(dT)-primed cDNA are shown in gray shades, those from random hexamer-primed cDNA in blue shades. Values shown are the means ± SE from three (Col-0 and *paps2-3 paps4-3*) or two (*paps1-1*) biological replicates, normalized to the constitutive reference gene *PDF2* (*AT1G13320*). Plants had been kept at 30 °C for 2 h before harvesting. $*P < 0.05$; $**P < 0.01$ (Student *t* test). (*C*) Bioanalyzer electropherogram of RT-PCR–amplified 3′ ends of *SAUR19/24* transcripts from the indicated genotypes. Two biological replicates per genotype are shown. RNA had been left untreated (*Left*) or poly(A) tails had been digested with RNAseH and oligo(dT) (*Right*) before reverse transcription. (*D*) Normalized signal intensities of the PCR products in *C*. Averages of the two biological replicates per genotype are shown. (*E*) Length distribution of poly(A) tails as determined by sequencing subcloned individual PCR products from intact RNA in *C*. *P* values in legend are from a Wilcoxon rank-sum test. (*F–H*) Leaf area (*F*), length (*G*), and width (*H*) of wild-type or *paps1-1* mutant plants with or without the *35S::GFP-SAUR19* transgene. Asterisks (*,**) indicate significant difference from value in the absence of the transgene at $P < 0.05$ (*) or $P < 0.01$ (**) according to *t* tests with Bonferroni correction.

type, *paps2-1 paps4-1*, and *paps1-1* were 22, 17, and 2 for *SAUR19/24* and 19, 20, and 2 for *SAUR62/63/66/68*, respectively. Measuring the *SAUR19/24* poly(A) tail length from nuclear RNA of wild-type and *paps1-1* inflorescences showed the same difference as seen for total RNA (Fig. S4 *A–C*), arguing that the shorter poly(A) tails are indeed due to defective nuclear polyadenylation, rather than faster cytoplasmic deadenylation in the mutant. The most parsimonious explanation of these results is that *SAUR* transcripts are polyadenylated directly and exclusively by the PAPS1 isoform.

We asked whether the phenotypic rescue of the *paps1* leaf-growth defect by the chimeric $PAPS4^{N}$-$PAPS1^{C}$ protein was mirrored at the molecular level by a rescue of the *SAUR* mRNA polyadenylation defect. The poly(A) tails on *SAUR19/24* mRNAs were longer in *paps1-1* plants expressing the chimeric $PAPS4^{N}$-$PAPS1^{C}$ protein than in plants expressing PAPS4 under the control of the *pPAPS1* promoter or in nontransgenic *paps1-1* mutants, yet they did not reach the wild-type length (Fig. S4 *D–F*). This indicates that the divergent C-terminal domains of the PAPS proteins influence the mapping of PAPS isoforms to at least some of their presumed targets, possibly via binding to different forms of 3′ end processing factors (3, 5).

Reduced *SAUR* Activity Contributes to the Leaf-Growth Defect in *paps1* Mutants. A recent report demonstrated that the activity of the *SAUR19-24* subfamily is required for normal cell expansion in hypocotyls and leaves (31). Hypocotyls in *paps1-1* are longer than in wild type (Fig. S5*A*), suggesting that other expansion-promoting effects override a possibly reduced *SAUR* activity in this organ. To determine whether reduced *SAUR19-24* activity contributed to the defect in leaf growth in *paps1-1* mutants, we introduced a *35S::GFP-SAUR19* transgene with the 3′ UTR of the *nopaline synthase* gene (*nos* terminator) into the mutant background. The transgene promoted growth, especially in the leaf-length direction, in both the wild-type and the *paps1-1* mutant background; however, it had a much stronger effect in the latter, both in absolute and in relative terms (leaf length +17% in wild-type, +38% in *paps1-1* background; Fig. 3 *F–H*). Indeed, leaf length was indistinguishable between *35S::GFP-SAUR19* and *paps1-1*; *35S::GFP-SAUR19* plants (Fig. 3*G*). This nonadditive effect indicates that the reduced leaf length in *paps1-1* mutants is due to lower *SAUR* activity, because otherwise the *GFP-SAUR19* transgene would be expected to have the same effect in both genetic backgrounds.

The above experiment suggests that SAUR19 protein levels are lower in *paps1-1* mutant than in wild-type leaves. However, the polyadenylation defect of *SAUR* mRNAs in *paps1* mutants does not seem to destabilize the mRNAs, as indicated by the qRT-PCR experiments on random hexamer-primed cDNA (Fig. 3*B*), as reported for several previous examples of stable mRNAs with very short poly(A) tails (32–34). Consistent with this, introducing the *dst2* mutant (35) into the *paps1-1* background to alleviate the inherent instability of *SAUR* mRNAs did not rescue the *paps1-1* phenotype (Fig. S5*B*). This suggests that in *paps1* mutants either nuclear export or translation efficiency of *SAUR* mRNAs is reduced, either of which could lead to reduced SAUR protein levels.

***paps1-1* Mutant Leaves Show a Constitutive Pathogen Response.** To identify additional biological processes affected by the *paps1* mutation, we compared the misregulated genes to more than 600 published *A. thaliana* microarray studies using MASTA (36). This identified a strong overlap with genes affected in the *constitutive expression of pathogenesis-related genes5* (*cpr5*) mutant and in response to pathogen infection and other stresses (Fig. 4*A* and Fig. S6*A*). In particular, the overlap was almost as strong with genes affected in *cpr5* vs. wild type as with genes affected in *cpr5 npr1* vs. *npr1*. This suggests that the constitutive pathogen response in *paps1-1* is independent of *NON-EXPRESSOR OF*

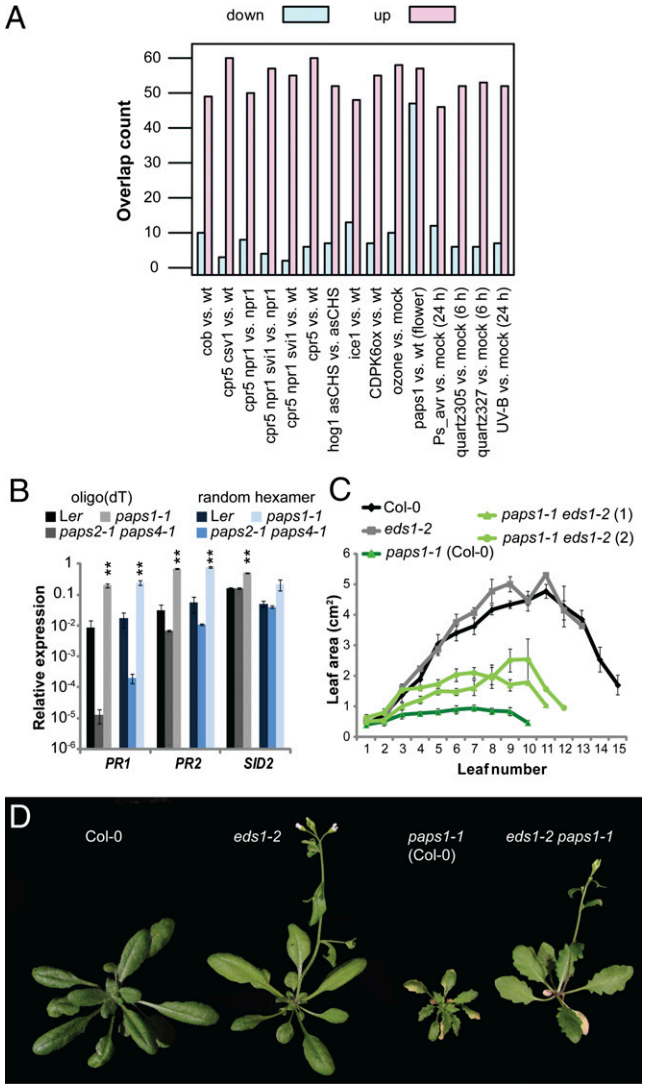

Fig. 4. Reduced leaf growth in *paps1* is partly due to an *EDS1*-dependent pathogen response. (*A*) Overlap of genes misregulated in leaves of *paps1-1* mutants vs. wild-type with genes misregulated in the experiments indicated. "Down" and "up" refer to the direction of the expression change in *paps1-1* vs. wild type. Table S3 defines the abbreviations used. (*B*) Expression of the indicated genes in *paps1-1* mutant seedlings compared with wild-type, using oligo (dT)-primed (gray shades) or random hexamer-primed cDNA (blue shades). Values shown are the means ± SE from three biological replicates, normalized to the constitutive reference gene *PDF2* (*AT1G13320*). (*C*) Quantification of leaf area in the indicated genotypes. Values shown are means ± SE from at least three plants per genotype. (*D*) Whole-plant phenotypes of the indicated genotypes.

PR1 (*NPR1*), a master regulator of the SA-mediated pathogen response (Fig. 4*A*) (37). This in turn suggests the activation of the *ENHANCED DISEASE SUSCEPTIBILITY1* (*EDS1*)/ *PHYTOALEXIN DEFICIENT 4* (*PAD4*)-dependent pathogen response in *paps1-1*, which forms part of the *cpr5* phenotype (38). The signature of a constitutive pathogen response was also evident at the single-gene level, with several classic marker genes specifically up-regulated in *paps1-1* mutant vs. wild-type leaves but not in *paps2-1 paps4-1* plants (e.g., *PR1*, *PR2*, *SID2*, and the defensins *PDF1.2b*, *PDF1.2c*, and *PDF1.4*) (Fig. 4*B* and Table S1).

Constitutive activation of the pathogen response results in reduced leaf growth due to reduced cell expansion (39). We therefore tested whether an *EDS1*/*PAD4*-dependent constitutive pathogen response contributes to the *paps1-1* phenotype. Indeed, leaf growth in the *eds1-2 paps1-1* and the *pad4-1 paps1-1* double mutants was substantially rescued (Fig. 4 *C* and *D* and Fig. S6 *B* and *C*). However, petal overgrowth was not rescued (Fig. S6*D*). Thus, an *EDS1*/*PAD4*-dependent constitutive pathogen response contributes to the reduced leaf growth but not to the petal overgrowth in *paps1* mutants. This indicates that *PAPS1*, but not *PAPS2* or *PAPS4*, negatively modulates the plant pathogen response. However, none of several pathogen-response associated genes tested (e.g., *EDS1*, *NPR1*, *PR1*, *PR2*, *SID2*, *SIZ1*, *WRKY18*), some of which are affected in the microarray analysis, showed a robust change in the lengths of their poly(A) tails.

Functional Specialization Among PAPS Isoforms Provides an Additional Level of Gene Regulation. Our results demonstrate that the three canonical nuclear PAPSs in *Arabidopsis* fulfill different functions owing to their divergent C-terminal domains. The very different mutant phenotypes, the results of analyzing bulk poly(A)-tail length, and the defects in polyadenylation of *SAUR* mRNAs in *paps1* but not *paps2 paps4* mutants strongly suggest that a fraction of transcripts is exclusively or preferentially targeted by PAPS1. As outlined in the Introduction, such target specificity provides an opportunity for regulating gene expression by modulating the balance of activities among the PAPS isoforms. PAPS1 is phosphorylated on several residues in its C-terminal domain [http://phosphat.mpimp-golm.mpg.de (40)], suggesting posttranslational modification as one way of altering PAPS1 activity. Reduced PAPS1 activity causes a constitutive pathogen response via an EDS1/PAD4-dependent mechanism. Thus, it is tempting to speculate that response to pathogen infection may be a scenario in which modulation of PAPS1 activity is used to alter the mRNA polyadenylation status and thus expression of a subset of pathogen-response factors. A genome-wide approach to determine poly (A) tail lengths will be required to identify the pathogen-response genes whose polyadenylation depends on PAPS1 to conclusively test this notion. Finally, we note that because homologs to PAPS1 and PAPS2/PAPS4 are found throughout higher plants in phylogenetically well-supported clades (17), this mode of regulation may function broadly in higher plants.

Materials and Methods

Plant Materials and Growth Conditions. The *paps1-1* mutation was identified in an EMS-mutagenesis screen in the Landsberg *erecta* (L*er*) background and back-crossed three times to L*er* before analysis. For comparison with mutants in the Col-0 background, the *paps1-1* mutation was introgressed into Col-0 by three rounds of back-crossing. Details of T-DNA insertion lines and other mutants used can be found in *SI Materials and Methods*.

Plant growth conditions were as described previously (41). All measurements were done with plants grown at 23 °C, unless otherwise stated. For the experiment involving the *35S::GFP-SAUR19* transgene plants were grown on 1/2 MS plates including 1% sucrose at 21 °C (day) and 14 °C (night).

Genotyping Mutant Alleles. For genotyping the *paps1-1* allele, a dCAPS marker (oSV126 and oSV166) was used. The PCR product (210 bp) from the mutated allele is cut by EcoRI. For genotyping of T-DNA insertion alleles, gene-specific primers (called LP and RP primer) that flank the T-DNA insertion site, and a T-DNA right border primer (BP) were used. These are listed in *SI Materials and Methods*.

Phenotypic Analysis, Measurements of Organ and Cell Sizes. Dissected organs were scanned, and their size was measured using ImageJ software (http://rsbweb.nih.gov/ij/). Petal-cell size was determined essentially as described previously (42). For determining cell size in leaves, leaves were fixed in FAA solution [10% (wt/vol) formaldehyde, 5% (vol/vol) acetic acid, 50% (vol/vol) ethanol], cleared with chloral hydrate, and observed using differential phase contrast. Further details can be found in *SI Materials and Methods*.

In Vitro Polyadenylation Assay and Measurement of Bulk Poly(A) Tail Length. Nonspecific polyadenylation assays were performed essentially as described previously (27), as was the measurement of bulk poly(A) tail lengths (43). Further details can be found in *SI Materials and Methods*.

Microarray Analysis. Transcriptomes of *paps1-1* mutant and wild-type seedlings and flowers (details in *SI Materials and Methods*) were compared using the Agilent *Arabidopsis* 4 × 44K oligo microarray. Two-color microarrays were normalized using the loess method (44). Differentially expressed genes were identified using the R/Bioconducor package Limma (45).

qRT-PCR and Measurements of Poly(A) Tail Length. Total RNA was prepared by the hot phenol method (46), DNase-digested, and reverse-transcribed using oligo$(dT)_{17}$ or random-hexamer primers. Expression levels were analyzed using a Roche LightCycler 480. Poly(A) tail length was determined using the Affymetrix Poly(A) Tail-Length Assay Kit. Details and primers used are described in *SI Materials and Methods*.

Molecular Cloning and Plant Transformation. The floral dip transformation protocol was carried out as described previously (47). Details of molecular cloning can be found in *SI Materials and Methods*.

ACKNOWLEDGMENTS. We thank Isabel Bäurle, Cyril Zipfel, and members of the Lenhard laboratory for discussion; Timothy Wells, Christiane Schmidt, and Doreen Mäker for excellent plant care; and Jane Parker and Pamela Green for seeds. S.L.V was supported by the Rotation PhD program from the John Innes Centre. Work in the M.L. laboratory was supported by Deutsche Forschungsgemeinschaft Grant Le1412/3-1. D.L. and T.L. were supported by Deutsche Forschungsgemeinschaft Grant La606/13-1 and the EU-INTEREG IV Upper Rhine program. W.M.G. was supported by National Institutes of Health (NIH) Grant GM067203 and National Science Foundation Grant MCB-0817205. N.R. and J.L.M. were supported by NIH Grant GM28983.

1. Eckmann CR, Rammelt C, Wahle E (2011) Control of poly(A) tail length. *Wiley Interdiscip Rev RNA* 2(3):348–361.
2. Hunt AG (2008) Messenger RNA 3′ end formation in plants. *Curr Top Microbiol Immunol* 326:151–177.
3. Millevoi S, Vagner S (2010) Molecular mechanisms of eukaryotic pre-mRNA 3′ end processing regulation. *Nucleic Acids Res* 38(9):2757–2774.
4. Proudfoot NJ (2011) Ending the message: Poly(A) signals then and now. *Genes Dev* 25(17):1770–1782.
5. Mandel CR, Bai Y, Tong L (2008) Protein factors in pre-mRNA 3′-end processing. *Cell Mol Life Sci* 65(7-8):1099–1122.
6. Schmidt MJ, Norbury CJ (2010) Polyadenylation and beyond: Emerging roles for noncanonical poly(A) polymerases. *Wiley Interdiscip Rev RNA* 1(1):142–151.
7. Lingner J, Kellermann J, Keller W (1991) Cloning and expression of the essential gene for poly(A) polymerase from S. cerevisiae. *Nature* 354(6353):496–498.
8. Raabe T, Bollum FJ, Manley JL (1991) Primary structure and expression of bovine poly (A) polymerase. *Nature* 353(6341):229–234.
9. Thuresson AC, Aström J, Aström A, Grönvik KO, Virtanen A (1994) Multiple forms of poly(A) polymerases in human cells. *Proc Natl Acad Sci USA* 91(3):979–983.
10. Juge F, Zaessinger S, Temme C, Wahle E, Simonelig M (2002) Control of poly(A) polymerase level is essential to cytoplasmic polyadenylation and early development in *Drosophila*. *EMBO J* 21(23):6603–6613.
11. Martin G, Keller W (2007) RNA-specific ribonucleotidyl transferases. *RNA* 13(11): 1834–1849.
12. Topalian SL, et al. (2001) Identification and functional characterization of neo-poly(A) polymerase, an RNA processing enzyme overexpressed in human tumors. *Mol Cell Biol* 21(16):5614–5623.
13. Kyriakopoulou CB, Nordvarg H, Virtanen A (2001) A novel nuclear human poly(A) polymerase (PAP), PAP gamma. *J Biol Chem* 276(36):33504–33511.
14. Zhao W, Manley JL (1996) Complex alternative RNA processing generates an unexpected diversity of poly(A) polymerase isoforms. *Mol Cell Biol* 16(5):2378–2386.
15. Kashiwabara S, et al. (2002) Regulation of spermatogenesis by testis-specific, cytoplasmic poly(A) polymerase TPAP. *Science* 298(5600):1999–2002.
16. Addepalli B, Meeks LR, Forbes KP, Hunt AG (2004) Novel alternative splicing of mRNAs encoding poly(A) polymerases in *Arabidopsis*. *Biochim Biophys Acta* 1679(2): 117–128.
17. Meeks LR, Addepalli B, Hunt AG (2009) Characterization of genes encoding poly(A) polymerases in plants: Evidence for duplication and functional specialization. *PLoS ONE* 4(11):e8082.
18. Hunt AG, et al. (2008) *Arabidopsis* mRNA polyadenylation machinery: Comprehensive analysis of protein-protein interactions and gene expression profiling. *BMC Genomics* 9:220.
19. Hunt AG, Meeks LR, Forbes KP, Das Gupta J, Mogen BD (2000) Nuclear and chloroplast poly(A) polymerases from plants share a novel biochemical property. *Biochem Biophys Res Commun* 272(1):174–181.
20. Di Giammartino DC, Nishida K, Manley JL (2011) Mechanisms and consequences of alternative polyadenylation. *Mol Cell* 43(6):853–866.
21. Ji Z, Lee JY, Pan Z, Jiang B, Tian B (2009) Progressive lengthening of 3′ untranslated regions of mRNAs by alternative polyadenylation during mouse embryonic development. *Proc Natl Acad Sci USA* 106(17):7028–7033.
22. Sandberg R, Neilson JR, Sarma A, Sharp PA, Burge CB (2008) Proliferating cells express mRNAs with shortened 3′ untranslated regions and fewer microRNA target sites. *Science* 320(5883):1643–1647.
23. Sherstnev A, et al. (2012) Direct sequencing of *Arabidopsis thaliana* RNA reveals patterns of cleavage and polyadenylation. *Nat Struct Mol Biol* 19(8):845–852.
24. Wu X, et al. (2011) Genome-wide landscape of polyadenylation in *Arabidopsis* provides evidence for extensive alternative polyadenylation. *Proc Natl Acad Sci USA* 108(30):12533–12538.
25. Murata T, et al. (2001) The hiiragi gene encodes a poly(A) polymerase, which controls the formation of the wing margin in *Drosophila melanogaster*. *Dev Biol* 233(1): 137–147.
26. Mellman DL, et al. (2008) A PtdIns4,5P2-regulated nuclear poly(A) polymerase controls expression of select mRNAs. *Nature* 451(7181):1013–1017.
27. Takagaki Y, Ryner LC, Manley JL (1988) Separation and characterization of a poly(A) polymerase and a cleavage/specificity factor required for pre-mRNA polyadenylation. *Cell* 52(5):731–742.
28. Liu F, Marquardt S, Lister C, Swiezewski S, Dean C (2010) Targeted 3′ processing of antisense transcripts triggers *Arabidopsis* FLC chromatin silencing. *Science* 327(5961): 94–97.
29. Chae K, et al. (2012) *Arabidopsis* SMALL AUXIN UP RNA63 promotes hypocotyl and stamen filament elongation. *Plant J* 71(4):684–697.
30. Hagen G, Guilfoyle T (2002) Auxin-responsive gene expression: Genes, promoters and regulatory factors. *Plant Mol Biol* 49(3-4):373–385.
31. Spartz AK, et al. (2012) The SAUR19 subfamily of SMALL AUXIN UP RNA genes promote cell expansion. *Plant J* 70(6):978–990.
32. Meijer HA, et al. (2007) A novel method for poly(A) fractionation reveals a large population of mRNAs with a short poly(A) tail in mammalian cells. *Nucleic Acids Res* 35(19):e132.
33. Gu H, Das Gupta J, Schoenberg DR (1999) The poly(A)-limiting element is a conserved cis-acting sequence that regulates poly(A) tail length on nuclear pre-mRNAs. *Proc Natl Acad Sci USA* 96(16):8943–8948.
34. Peng J, Schoenberg DR (2005) mRNA with a <20-nt poly(A) tail imparted by the poly (A)-limiting element is translated as efficiently in vivo as long poly(A) mRNA. *RNA* 11(7):1131–1140.
35. Johnson MA, Perez-Amador MA, Lidder P, Green PJ (2000) Mutants of *Arabidopsis* defective in a sequence-specific mRNA degradation pathway. *Proc Natl Acad Sci USA* 97(25):13991–13996.
36. Reina-Pinto JJ, Voisin D, Teodor R, Yephremov A (2010) Probing differentially expressed genes against a microarray database for in silico suppressor/enhancer and inhibitor/activator screens. *Plant J* 61(1):166–175.
37. Dong X (2004) NPR1, all things considered. *Curr Opin Plant Biol* 7(5):547–552.
38. Clarke JD, Aarts N, Feys BJ, Dong X, Parker JE (2001) Constitutive disease resistance requires EDS1 in the *Arabidopsis* mutants cpr1 and cpr6 and is partially EDS1-dependent in cpr5. *Plant J* 26(4):409–420.
39. Bowling SA, et al. (1994) A mutation in *Arabidopsis* that leads to constitutive expression of systemic acquired resistance. *Plant Cell* 6(12):1845–1857.
40. Durek P, et al. (2010) PhosPhAt: The *Arabidopsis thaliana* phosphorylation site database. An update. *Nucleic Acids Res* 38(Database issue):D828–D834.
41. Disch S, et al. (2006) The E3 ubiquitin ligase BIG BROTHER controls *Arabidopsis* organ size in a dosage-dependent manner. *Curr Biol* 16(3):272–279.
42. Horiguchi G, Fujikura U, Ferjani A, Ishikawa N, Tsukaya H (2006) Large-scale histological analysis of leaf mutants using two simple leaf observation methods: Identification of novel genetic pathways governing the size and shape of leaves. *Plant J* 48(4):638–644.
43. Preker PJ, Lingner J, Minvielle-Sebastia L, Keller W (1995) The FIP1 gene encodes a component of a yeast pre-mRNA polyadenylation factor that directly interacts with poly(A) polymerase. *Cell* 81(3):379–389.
44. Smyth GK, Speed T (2003) Normalization of cDNA microarray data. *Methods* 31(4): 265–273.
45. Smyth GK (2004) Linear models and empirical Bayes methods for assessing differential expression in microarray experiments. *Stat Appl Genet Mol Biol* 3(1):Article 3.
46. Box MS, Coustham V, Dean C, Mylne JS (2011) Protocol: A simple phenol-based method for 96-well extraction of high quality RNA from *Arabidopsis*. *Plant Methods* 7:7.
47. Clough SJ, Bent AF (1998) Floral dip: A simplified method for Agrobacterium-mediated transformation of *Arabidopsis thaliana*. *Plant J* 16(6):735–743.